EFFECTS OF SODIUM, POTASSIUM AND CALCIUM CHLORIDE SALTS ON UNDERWATER VISIBLE LIGHT COMMUNICATION PERFORMANCE AND THEIR PRESENCE IN SOME WATER BODIES OF SOUTHWEST NIGERIA

OLAOYE KOLAWOLE[1]*, PONNLE AKINLOLU[1], OJEDIRAN ARIKE[2]

[1] Department of Electrical and Electronics Engineering, Federal University of Technology, Akure, Nigeria.
[2] Department of Information and Communication Engineering, Federal University of Technology, Akure, Nigeria.
* Correspondence: kolawoleolaoye071740@gmail.com

Received: date 19.02.2024
Revised: date 27.01.2025
Accepted: date 06.03.2025
Published: date 26.06.2025

Abstract: The Salinity is one of the attributes of water that affects underwater wireless optical communication (UWOC) and requires continual investigation. This study investigates the effect of sodium, potassium and calcium chloride salts on transmission of visible light in water via spectroscopy for underwater communication, as well as the presence of these salts in seven water bodies of Southwest Nigeria. Single-salt solutions of each type with varying concentrations were prepared, and their physiochemical properties were measured, as well as their visible light absorbance spectra, from which performance of UWOC for each salt solution at three wavelengths was investigated by simulation using OptiSystem. Water samples were taken from three rivers, two lagoons, and the Atlantic Ocean in Southwest Nigeria and the concentration of the three cations and chloride ion in them were measured as well as their absorbance spectra. For the single-salt solutions, higher absorbance at shorter wavelengths was observed with an increase in salt concentration for sodium and potassium chloride solutions, but calcium chloride solution shows higher absorbance towards longer wavelengths. UWOC simulation results showed that the achievable maximum link distance reduces with salt concentration, varies with wavelength, and is least in calcium chloride solution. For the water bodies, the rivers have low values of salinity and absorbance, while high values were obtained for the lagoons and the Atlantic Ocean. Moreover, their average absorbance showed strong correlations with concentration of calcium and chloride ions than with sodium and potassium ions.

Keywords: salinity, sodium chloride, potassium chloride, calcium chloride, absorbance, underwater wireless optical communication

1. INTRODUCTION

Underwater wireless optical communication (UWOC) is a communication technology that offers a high data capacity for communicating underwater using light [1]. It enables high-speed and secure communication over short

* Corresponding author, email: kolawoleolaoye071740@gmail.com https://doi.org/10.29081/jesr.v30i4.004

and medium distances underwater. However, the natural underwater environment is a complex and continually changing environment to light.

UWOC is adversely affected by absorption and scattering. Absorption occurs when photons lose energy to other forms as a result of interaction with water molecules and other particles in the water [2, 3]. Scattering occurs when photons are deflected from their original path after interacting with particles in the water. This may cause beam spreading and distortions which results in inter-symbol interference and poor system's performance [4].

Salinity is among the factors that significantly influence the performance of UWOC systems. It affects the refractive index, absorption, and scattering properties of water, which, in turn, influence the propagation of light underwater. Dissolved salt in water brings about salinity. In all the oceans of the world, salinity is different for different layers [5]. Changes in the optical properties of water affect the transmission of optical signals in it and the received power [6]. The study of authors in [7] on UWOC channels showed that increasing sea salt concentrations brings about increase of light attenuation and strongly affects the performance of the UWOC system. Sodium chloride (NaCl), potassium chloride (KCl), and calcium chloride ($CaCl_2$) are salts which are highly soluble in water. They, and other salts such as calcium sulfate ($CaSO_4$), magnesium sulfate ($MgSO_4$), magnesium chloride ($MgCl_2$), and sodium bicarbonate ($NaHCO_3$), contribute mainly to attenuation of optical signals underwater [8].

Many researchers have carried out experimental studies on the optical properties of water to salts [9 – 12]. Authors in [13] showed that in solutions of NaCl, Na_2SO_4, and $MgCl_2$ to light within 430 nm - 630 nm, the variations in optical attenuation have much to do with the suspended particles than with the dissolved substances in the solution. However, their study did not include KCl and $CaCl_2$.

Authors in [14] studied UWOC performance in saline water of varying concentrations in vertical channel of water. Attenuation increased with salinity, and with reduced link distance. However, only one type of salt solution was experimented with.

Authors in [15, 16], used spectroscopy to study different concentrations of NaCl and KCl single-salt and dual-salt solutions from ultraviolet to near infrared. NaCl and KCl have similar behaviors in the visible range but with marked different behavior in the infrared. Authors in [17] studied absorption effect of different concentrations of NaCl, KCl, $MgSO_4$, $MgCl_2$, and $NaHCO_3$ from 200 nm – 1200 nm using a UV spectrophotometer. However, they did not include $CaCl_2$ in their study.

Authors in [18] studied extinction coefficients of NaCl, $MgCl_2$, Na_2SO_4, KCl, and $CaCl_2$ multi-component mixed-salt solutions within the range 300 nm – 1000 nm. Their work centered on solutions of mixture of the salts in various proportions and weight ratios, and not single-salt solutions.

Authors in [19, 20] studied the transmission of visible light via spectroscopy in the range 400 nm - 800 nm in water containing common table salt of different concentrations, and its attenuation effect on UWOC. The study is however limited to only sodium chloride water.

Southwest Nigeria is within the rain forest belt of the country, with uplands in the northern part of the region, and lagoons and the Atlantic Ocean in the southern part where Lagos is located. Lagos is a large metropolitan city and a major economic hub of Nigeria. Many rivers in the Southwest Nigeria flow from the uplands towards the Atlantic Ocean in Lagos, thus it becomes expedient to study its waters for UWOC. The study of absorbance of the water bodies in the Southwest Nigeria to visible light spectrum for optical communication purposes is still scanty, even though some researchers have studied some physiochemical properties of some of these waters [21 – 23].

Authors in [24] carried out a study on the transmission of visible light from 400 nm - 800 nm in ten natural water bodies of Southwest Nigeria via spectroscopy. The water bodies include rivers, lagoons and the Atlantic Ocean. The study helps determine the most suitable wavelength for visible light communication across these selected natural water bodies at minimal attenuation. However, the salt ionic contents of these water bodies were not investigated.

The purpose of this paper is to investigate the salt ionic contents of the water bodies of Southwest Nigeria with respect to UWOC performance. In this paper, the salts investigated were limited to sodium chloride (NaCl), potassium chloride (KCl), and calcium chloride ($CaCl_2$) which are salts that are highly soluble in water. First,

visible light attenuation in single-salt solutions of these salts of different concentrations was investigated by spectroscopy and measurement of physiochemical properties, and their consequent effect on performance of underwater visible light communication. Then, seven natural water bodies among those studied by [24] were selected to investigate the presence of these salts in them and their effects on transmission of visible light in the waters. The amounts of sodium, potassium, calcium and chloride ions in them were measured for correlations with their light absorption.

The rest of the paper is organized as follows: Section 2 briefly discusses salinity and underwater optical communication. Section 3 presents and discusses the materials and methods used in the measurement of the physiochemical parameters of the salt solutions and light absorbance, as well as the UWOC simulation; the measurement of the physiochemical properties and light absorbance of the water bodies; and the determination of the three cations (metallic ions) and chloride ions in them. Section 4 presents and discusses the results, and finally conclusion is made in Section 5.

2. SALINITY AND UWOC

2.1. Salinity

Salinity is a measure of all the total salts dissolved in water, usually expressed in parts per thousand or parts per million. It can be determined from chloride ion concentration by the expression in equation (1).

$$S = \beta Cl^{-} \tag{1}$$

where S is the salinity (ppt), Cl^{-} is the chloride ion concentration (mg/L), and β = 0.00180665.

Adding salt to water changes the absorption spectrum of water. NaCl (aq), KCl (aq), and $CaCl_2$ (aq) do not absorb much in the visible range, but they show some significant absorption features in the ultraviolet and infra-red range [25]. Aqueous solutions of sodium and potassium chloride show similar absorbance spectra [15].
Beer's Law relates the absorbance, A to the concentration, C of a solution. The Law is written as in equation (2):

$$A = \varepsilon l C \tag{2}$$

where ε is the molar absorptivity which is wavelength-dependent and varies for different solutions; and l is the path length of light through the solution.

2.2. Underwater optical communication performance

Absorption and scattering contribute mainly to the attenuation of light in water [26]. Absorption is the loss or transfer of photon energy when it interacts with water molecules, dissolved organic matters and other particles in the water [2]. In scattering, the path of the photons changes from their initial path after interacting with particles in the water without the loss of energy. If the size of the particles in the water is comparable to the wavelength of light, diffraction occurs, and if the refractive index of the particles is different from the refractive index of the water, then refraction takes place [27]. A parameter which is referred to as attenuation coefficient of the medium c(λ), is used to represent the combined effect of absorption and scattering, and is expressed as in equation (3):

$$c(\lambda) = a(\lambda) + b(\lambda) \tag{3}$$

where a(λ) is the spectral absorption coefficient, b(λ) is the spectral scattering coefficient, and λ is the wavelength.

When light enters into water, a portion of the incident power is absorbed in the water, a portion is scattered, and the remaining is transmitted through the water. In UWOC, Beer Lambert's law relates the power of a light beam in a medium to the attenuation and the distance the light traveled from the optical transmitter, which is as expressed in equation (4):

$$P(x) = P_T e^{-c(\lambda)x} \tag{4}$$

where P_T is the initial optical power from the transmitter, $P(x)$ is the transmitted optical power at distance x from the transmitter, and c(λ) is the attenuation coefficient of the medium as expressed in Equation (3). Since the

attenuation coefficient varies with wavelength, therefore the transmitted power is also wavelength-dependent. Attenuation reduces the transmission range and signal quality.

3. EXPERIMENTAL SETUP

3.1. Preparation and salinity measurement of the single-salt solutions

Separate single-salt solutions of eight different concentrations of NaCl, $CaCl_2$ and KCl were prepared. The salts were obtained from the Department of Chemistry of the authors' institution. Each of the salt samples was weighed to determine the amount of concentration for each of the salt solution. Salt weights of 1 g, 3 g, 5 g, 10 g, 15 g, 20 g, 25 g and 30 g using an electronic analytical balance (model FA2104A from Shanghai Jingtian Electronic Instrument Co. Ltd.) to weigh the salts, were each dissolved in 100 ml of de-ionized water with electrical conductivity of 0.2 µS/cm. The electrical conductivity, total dissolved salt (TD salt) and total dissolved solids (TDS) of each salt solution were measured using a digital water quality tester EZ-9909SP as explained in [24].

3.2. Measurement of absorbance in samples

A VIS-721 Visible Light Spectrophotometer was used to determine the absorption of the three salt solutions in the visible light range. The procedure for this measurement is as explained in [20]. The measurements were made at a wavelength interval of 50 nm, from 400 nm – 800 nm. From these measurements, average absorbance for each type of salt solution at different concentrations was evaluated, and consequently their absorptivity was evaluated at each wavelength using equation (2).

The average absorbance for each type of salt solution at a given concentration Av_c, is given by equation (5):

$$A_{Vc} = \frac{\sum_{i=1}^{K} A(\lambda_i)}{K} \tag{5}$$

where $A(\lambda_i)$ is the measured absorbance at wavelength i, and K is the total number of wavelengths of measurements which is nine in this case.

3.3. Underwater wireless optical communication simulation

Using the absorption coefficient evaluated from absorbance values for each sample, performance of UWOC link for each sample with a continuous laser beam of 30 mW at selected wavelengths of 450 nm, 550 nm, and 700 nm; and at a data rate of 1 Gb/s was simulated using OptiSystem software linked with MATLAB. The performance was evaluated in terms of maximum link distance achievable for the maximum allowable bit error rate (BER) in UWOC of 10^{-9} [28]. Quality factor (QF) was also determined. The simulation parameters used in the simulation are shown in Table 1, and the schematic layout of the UWOC in OptiSystem is shown in Figure 1.

Table 1. Simulation parameters.

Parameters	Values
Operating wavelength of laser	450 nm, 550 nm and 700nm
Power of Laser	30 mW
Bit rate of bit sequence generator	10 Gbps
Modulation	NRZ OOK
Amplitude of NRZ pulse generator	1 a.u.
Modulation index of amplitude modulator	1
Responsivity of photodetector	1 A/W
Dark current of photodetector	10 nA
Cutoff frequency of filter	0.75 x Bit rate

In Figure 1, the Pseudo-Random Bit Sequence (PRBS) generator produces random bit sequences at a bit rate of 1 Gbps which is passed to the Non-Return to Zero (NRZ) Pulse Generator to produce a sequence of random rectangular NRZ electrical pulses. A continuous wave (CW) laser beam at the determined wavelengths and power, is passed to an Amplitude Modulator (AM) which uses the NRZ electrical pulses to modulate the CW laser in order to produce a modulated optical output signal. The underwater optical channel is represented by a MATLAB code that is linked with the Optisystem, which receives the modulated optical signal from the modulator and

attenuates it within the channel. The attenuated optical signal is then received by the PIN Photodiode which gives an electrical output signal. The Low Pass Gaussian Filter reduces the noise, before being passed to the Eye Diagram Analyzer through the 3R Regenerator. The eye diagram analyzer shows the recovered electrical signals, from which the QF and the BER can be determined.

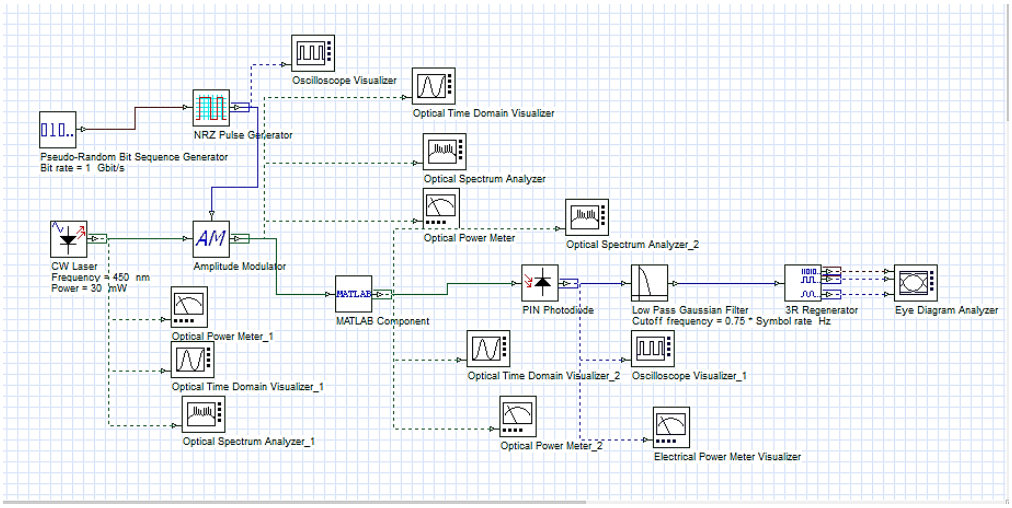

Fig. 1. Layout of the UWOC in OptiSystem.

3.4. Physiochemical parameters and light absorbance measurement of the natural water bodies

Samples of the seven selected water bodies of Southwest Nigeria investigated in this study were from the Atlantic Ocean (AO), Lagos Lagoon Victoria Island (LLVI), Lagos Lagoon Lekki Phase 1 (LLLP1), Epe Lagoon (EL), Apake River, Ala River, and Ogbese River. The description of the water bodies, locations, procedure of samples collection, the procedure of measurement of their physiochemical properties, and light absorbance within 400 nm - 800 nm via spectroscopy followed as explained in [24]. The average absorbance for each water body was also computed using equation (5).

3.5. Measurement of sodium, potassium, calcium, and chlorine ions in the water bodies

3.5.1. Determination of metallic ions in the water samples

The instrument used for determination of the concentration of metallic ions (cations) in the samples is the flame photometer (model FP910) from PG Instruments Limited. It gives fast, accurate measurements and precise analysis of sodium, potassium, calcium and lithium in a single aspiration [29]. It is a controlled flame test in which the intensity of the color of the flame is quantified. The intensity depends on the absorbed energy by the atoms enough to vaporize them. The instrument was first calibrated by standard solutions of the ions to be measured. The samples were then introduced to the flame at a constant rate, and filters select which color the photometer detects to the exclusion of the influence of other ions.

3.5.2. Determination of chloride ion concentration in the water samples

The Mohr's method [30] was used to determine the chloride ion concentration in the water samples by titration with Silver Nitrate ($AgNO_3$).

A. Materials and Reagents:

a) Potassium Chromate (K_2CrO_4) solution was used as an indicator. The solution was prepared by dissolving 5g of K_2CrO_4 in de-ionized water and distilled to 100 ml.
b) 0.1M of $AgNO_3$ solution was prepared by dissolving 17g of $AgNO_3$ crystals in 1L of distilled water.
c) Calcium Carbonate ($CaCO_3$) powder.

B. Procedure:

The water samples were first filtered to remove dirt and seaweeds. The procedure as described in [31] was followed involving the water samples, K_2CrO_4, $CaCO_3$ and $AgNO_3$. It also included a blank titration by substituting the water sample with de-ionized water. As the silver nitrate was being added to the water samples, silver chloride (AgCl) was precipitated. More Ag^+ reacted with the CrO_4^{2-} to form a precipitate of silver chromate (Ag_2CrO_4). The chemical equations of reactions are as expressed in equation (6) and equation (7):

$$Ag^{+}_{(aq)} + Cl^{-}_{(aq)} \rightarrow AgCl_{(s)} \quad (6)$$

$$2Ag^{+}_{(aq)} + {CrO_4}^{2-}_{(aq)} \rightarrow Ag_2CrO_{4(s)} \quad (7)$$

The chloride ion content in a sample is expressed as in equation (8) [31]:

$$Cl^{-}_{(mg/L)} = \frac{70{,}900(B-D)M}{V_s} \quad (8)$$

where B is the volume of the $AgNO_3$ for the water sample, D is the volume of the $AgNO_3$ for the blank titration, M is the molarity of the $AgNO_3$, and V_s is the volume of the sample.

4. RESULTS AND DISCUSSION

4.1. Results of salinity measurement of the single-salt solutions

Table 2 shows the measured physiochemical parameters for the three salt solutions of sodium chloride, potassium chloride and calcium chloride. Their electrical conductivity (EC), TDS, and TD salt increase as their concentration increases.

Table 2. Measured parameters for the NaCl, KCl, and $CaCl_2$ solutions.

Conc. (g/100 ml)	NaCl			KCl			$CaCl_2$		
	EC (mS/cm)	TD Salt (ppt)	TDS (ppt)	EC (mS/cm)	TD Salt (ppt)	TDS (ppt)	EC (mS/cm)	TD Salt (ppt)	TDS (ppt)
1.0	17.8	8.9	9.9	18.8	10.9	11.3	20.0	12.0	13.4
3.0	58.8	29.4	36.2	59.8	30.8	38.2	60.0	32.0	40.2
5.0	83.8	41.9	52.9	85.8	42.0	54.0	87.0	44.0	56.0
10.0	96.2	48.4	63.0	98.2	50.4	65.0	100.0	52.4	67.0
15.0	196.8	97.4	147.9	198.8	99.4	149.9	200.0	101.6	151.0
20.0	223.3	111.7	170.6	225.3	113.8	172.8	230.2	115.0	174.0
25.0	243.1	121.6	187.2	245.2	123.8	189.3	250.3	125.0	191.3
30.0	250.0	125.0	193.0	252.1	127.0	195.0	255.2	129.0	197.0

In Table 2, it can be observed that all the three salt solutions follow the same trend as their conductivity, TD salt and TDS increase with concentration. Moreover, at each concentration value, the three salt solutions have close conductivity, TD salt and TDS values. Those of calcium chloride solution are the highest, followed by potassium chloride solution, while sodium chloride solution has the least values. Figure 2 shows the plots of TDS and TD salt against conductivity for the three single-salt solutions. The TD salt has a linear relationship with the electrical conductivity; and the TDS shows a strong positive correlation with conductivity.

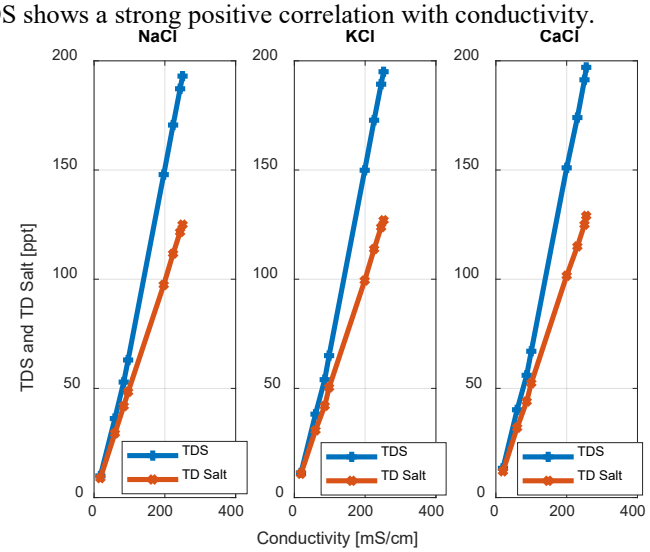

Fig. 2. Plots of TDS and TD Salt against conductivity for the three salt solutions.

4.2. Absorbance measurement results of the single-salt solutions

In this section, the results of the absorbance measurements of the three single-salt solutions within visible wavelength of 400 nm - 800 nm are presented and discussed.

4.2.1. Results for sodium chloride solution

Figure 3 shows the graph of absorbance against wavelength between 400 nm – 800 nm for NaCl solution at different levels of concentration.

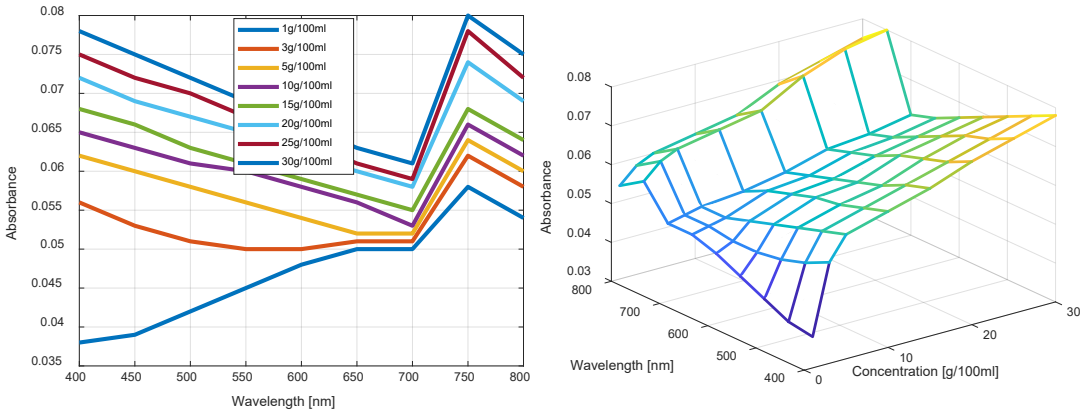

Fig. 3. Absorbance vs wavelength for the NaCl solution at different concentrations (a) 2-D Plot, (b) 3-D Plot.

Firstly, it can be observed that at all wavelengths, the absorbance increases with increase in the concentration. Secondly, the absorbance spectra do not show same pattern for all concentrations. At 1g/100 ml concentration, there is less attenuation at the short wavelengths (400 - 600 nm) than at the longer wavelengths (600 – 700 nm) which show more attenuation. Between 700 – 750 nm, the absorbance increases further but reduces between 750 – 800 nm. This pattern is close to that of pure water as already reported in literature [17]. In contrast, at higher salt concentrations of 3g/100ml to 30g/100ml, there are more attenuation at the short wavelengths (400 - 450 nm) and reduce towards the longer wavelengths (650 - 700 nm). Towards infra-red (700 – 750 nm), the absorbance increases while there is a reduction in the absorbance between 750 – 800 nm.

In general, the results of the absorbance measurements of the NaCl solution in this work agree with that of [20] except of slight deviation for concentration of 1 g/100ml. The salts used in this work were chemically produced in the laboratory, but the sodium chloride used and reported in [20] was common table salt containing some quantities of iodine and anti-caking agent.

4.2.2. Results for potassium chloride solution

Figure 4 shows the graph of absorbance against wavelength between 400 nm – 800 nm for KCl solution at different levels of concentration.

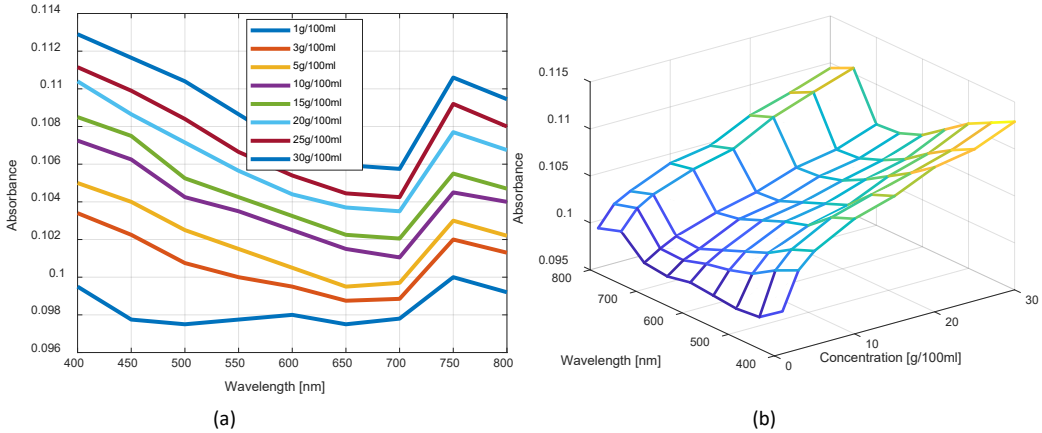

Fig. 4. Absorbance vs. wavelength for the KCl solution at different concentrations (a) 2-D Plot, (b) 3-D Plot.

The figure shows that apart from increase in absorbance with concentration, the absorbance spectra shows resemblance to that of the NaCl solution, except that the absorbance values of the KCl solution are slightly higher than those of the NaCl for corresponding concentrations and wavelengths. Also, at 1g/100 ml concentration, the absorbance shows almost a constant value between 450 nm – 700 nm, and then increases towards the infra-red.

4.2.3. Results for calcium chloride solution

Figure 5 shows the graph of absorbance against wavelength between 400 nm – 800 nm for the $CaCl_2$ solution at different levels of concentration.

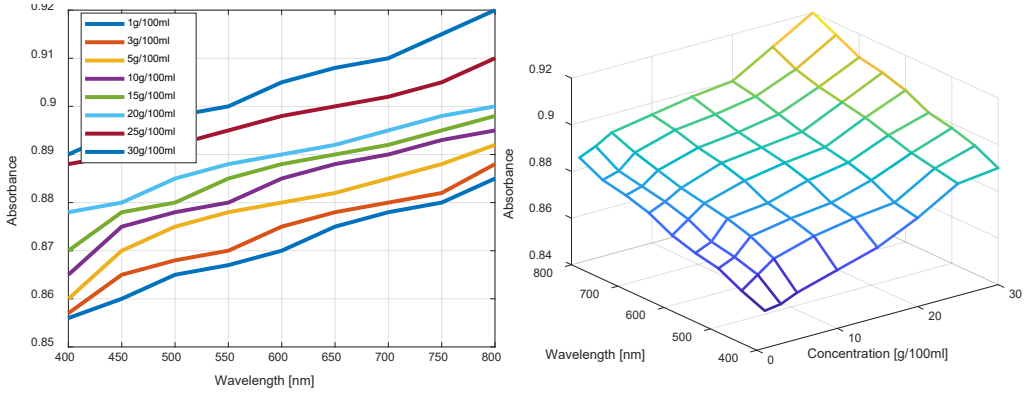

(a) (b)

Fig. 5. Absorbance vs wavelength for the $CaCl_2$ solution at different concentrations (a) 2-D Plot, (b) 3-D Plot.

The results for the $CaCl_2$ solution show different absorbance spectra to that of KCl and NaCl solutions. Apart from increase in absorbance with concentration, there is noticeable increase in absorbance as the wavelength increases. This implies that there is higher attenuation towards the longer wavelengths than at shorter wavelengths in this solution. Also, the absorbance values are much larger than those for the KCl and NaCl solutions.

4.2.4. Average absorbance and absorptivity

Figure 6(a) shows the plot of average absorbance against concentration for all the three single-salt solutions computed using Equation (5), and Figure 6(b) shows the absorptivity obtained at different wavelengths for them.

In Figure 6(a), the $CaCl_2$ solution has the highest average absorbance, followed by the KCl solution while the NaCl solution has the least values. Average absorbance of the KCl and NaCl solutions are close in values. It can also be observed that for each salt solution, average absorbance increases with salt concentration. This agrees with [15] and [20].

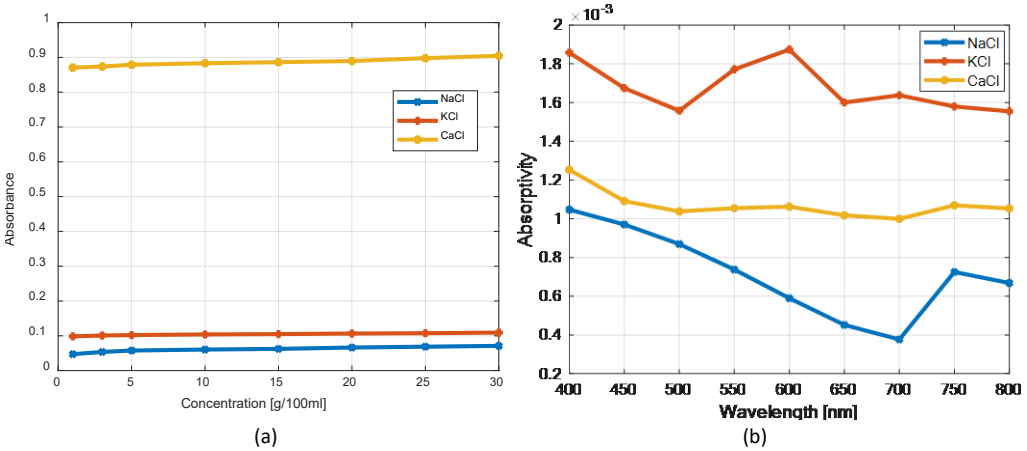

(a) (b)

Fig. 6. (a) Plot of average absorbance with concentration for all the three salt solutions. (b) Absorptivity of the three salt solutions between 400 nm – 800 nm

The absorptivity at a particular wavelength, which is as defined in equation (2), indicates that it is the rate of change of the absorbance with concentration per unit path length at that wavelength. In Figure 6(b), the absorptivity is highest at 400 nm (blue light) and reduces gradually towards the longer wavelengths (red and infra-red light) for all the three single-salt solutions. For NaCl solution, the absorptivity has the least value at 700 nm; this indicates that the absorbance of the solution has the least rate of change to concentration at this wavelength. A practical implication of this is that for light at this wavelength in a body of sodium chloride water, if the concentration of the salty water changes by a wide magnitude, the light absorbance changes by a small margin, and therefore it would be best to transmit light at this wavelength in the water. Considering Figure 6(b) again, it is worthy of note that of the three salt types, the KCl solution has the highest absorptivity spectrum despite that it does not have the highest average absorbance; followed by the $CaCl_2$ solution, and the least by NaCl solution. This implies that of the three salt solutions within 400 nm – 800 nm, light absorbance of KCl solution changes markedly to changes in concentration than the other two salt solutions. As was presented, it has highest rates of change at 400 nm and 600 nm. Another observation in Figure 6(b) is that $CaCl_2$ solution has fairly constant rate of change of absorbance across the spectrum, while NaCl solution shows the widest variation in rate of change of absorbance across the spectrum.

4.3. UWOC simulation and performance

This section presents the results of the simulation in terms of achievable maximum link distance for the maximum allowable BER in UWOC of 10^{-9} at 450 nm, 550 nm and 700 nm for the different single-salt solutions at the selected concentrations. For the three salt solutions, the maximum link distance reduces considerably as the salinity increases for the three wavelengths. Table 3 shows the BER and QF obtained from the simulation yielding the distances indicated for NaCl, KCl and $CaCl_2$ solutions in Figure 7 (a), (b), and (c) respectively.

Table 3. Results of Simulation for BER of 10^{-9} at 450 nm, 550 nm, and 700 nm for NaCl, KCl, and $CaCl_2$ solutions.

Wavelength (nm)	Concentration (g/100ml)	NaCl		KCl		$CaCl_2$	
		BER	QF	BER	QF	BER	QF
450	1	1.61×10^{-9}	5.97	3.56×10^{-9}	5.79	1.57×10^{-9}	5.92
	3	1.08×10^{-9}	5.98	3.29×10^{-9}	5.80	2.18×10^{-9}	5.86
	5	4.81×10^{-9}	5.73	1.20×10^{-9}	5.96	3.52×10^{-9}	5.79
	10	5.49×10^{-9}	5.71	1.93×10^{-9}	5.88	2.61×10^{-9}	5.84
	15	3.28×10^{-9}	5.80	1.33×10^{-9}	5.94	3.96×10^{-9}	5.77
	20	3.11×10^{-9}	5.80	1.28×10^{-9}	5.92	1.72×10^{-9}	5.91
	25	5.5×10^{-9}	5.77	2.35×10^{-9}	5.85	2.66×10^{-9}	5.84
	30	2.16×10^{-9}	5.87	1.60×10^{-9}	5.92	2.15×10^{-9}	5.87
550	1	1.78×10^{-9}	5.90	5.81×10^{-9}	5.66	1.77×10^{-9}	5.90
	3	3.14×10^{-9}	5.81	1.55×10^{-9}	5.92	1.23×10^{-9}	5.96
	5	3.98×10^{-9}	5.77	7.26×10^{-9}	5.66	2.16×10^{-9}	5.87
	10	1.02×10^{-9}	5.99	1.38×10^{-9}	5.94	2.96×10^{-9}	5.82
	15	1.25×10^{-9}	5.96	5.40×10^{-9}	5.71	4.25×10^{-9}	5.76
	20	3.26×10^{-9}	5.80	1.89×10^{-9}	5.86	1.13×10^{-9}	5.98
	25	1.08×10^{-9}	5.98	2.73×10^{-9}	5.83	1.15×10^{-9}	5.93
	30	2.16×10^{-9}	5.90	2.00×10^{-9}	5.88	3.96×10^{-9}	5.77
700	1	1.22×10^{-9}	5.96	8.44×10^{-9}	5.61	1.98×10^{-9}	5.89
	3	3.13×10^{-9}	5.81	6.65×10^{-9}	5.68	3.92×10^{-9}	5.77
	5	5.85×10^{-9}	5.70	4.94×10^{-9}	5.73	1.27×10^{-9}	5.96
	10	2.7×10^{-9}	5.83	1.60×10^{-9}	5.91	2.29×10^{-9}	5.86
	15	2.18×10^{-9}	5.87	4.25×10^{-9}	5.76	1.49×10^{-9}	5.93
	20	3.77×10^{-9}	5.77	4.82×10^{-9}	5.74	3.62×10^{-9}	5.78
	25	1.04×10^{-9}	5.99	2.52×10^{-9}	5.84	3.14×10^{-9}	5.81
	30	2.59×10^{-9}	5.84	1.35×10^{-9}	5.94	3.56×10^{-9}	5.79

It can be observed from Figure 7(a) that for the NaCl solution, the maximum link distance of 85 cm was achievable for the 1g/100 ml concentration at 450 nm, while maximum link distance of 66 cm was achievable at 700 nm. However, as the salinity increases from 3g/100 ml and beyond, 700 nm gave the highest maximum link distance while 450 nm gave the least maximum link distance.

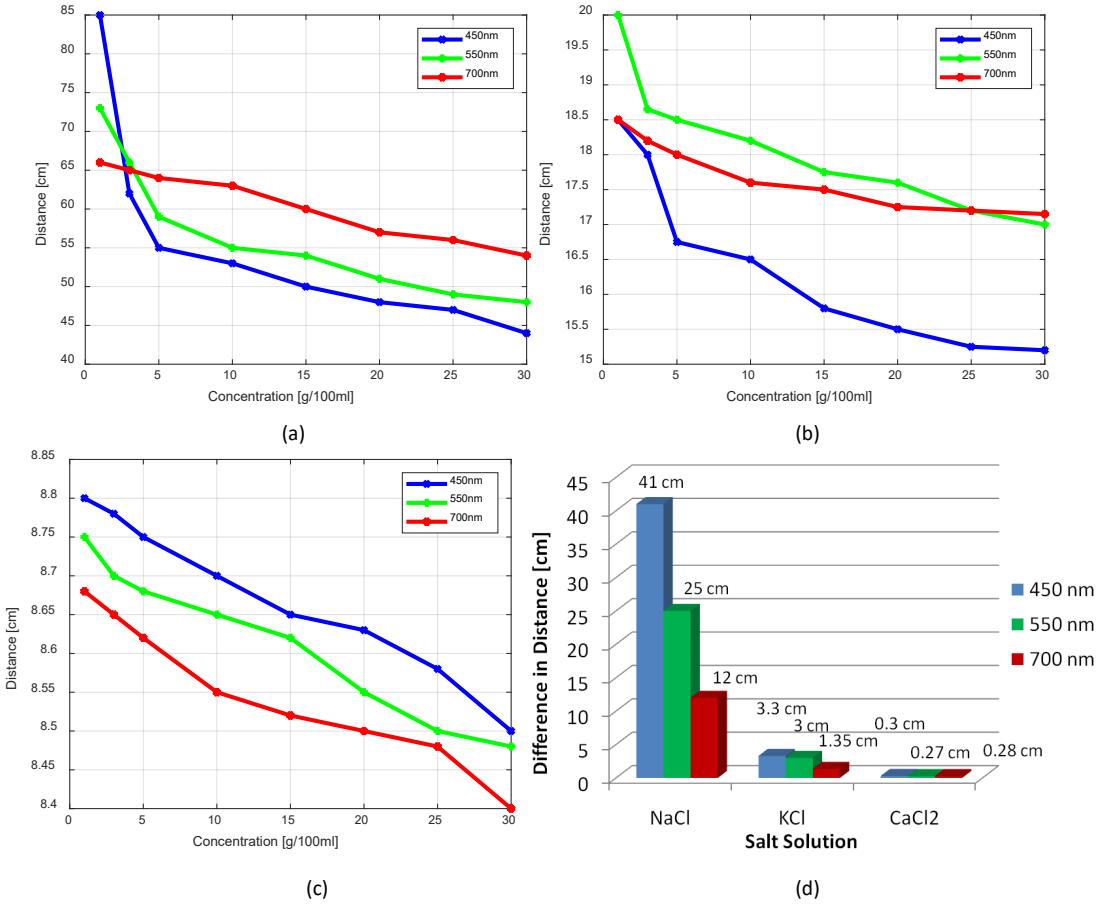

Fig. 7. Simulation results for maximum link distance achievable for the maximum allowable BER for (a) NaCl water, (b) KCl water, (c) $CaCl_2$ water. (d) Difference in maximum link distance at the three wavelengths for concentration between 1g/100ml and 30g/100ml for the three salt solutions.

For KCl solution (Figure 7(b)), 550 nm gave the highest maximum link distance while 450 nm gave the least maximum link distance for most of the salt concentrations. This implies that transmission around the green region will be most suitable for KCl water except at very high concentration levels in which red light will be a better choice for transmission. The actual link distances are shorter compared to those of the NaCl solution.

For $CaCl_2$ solution (Figure 7(c)), the highest maximum link distance is at 450 nm while the least maximum link distance is at 700 nm for all the salt concentrations. However, it should be noted that the actual link distances are very small compared to those of the NaCl and KCl solutions. Also, the link distances for the $CaCl_2$ solution are somewhat close in values.

This brings a notable observation which is the difference in maximum link distance at the three wavelengths for concentration between 1g/100ml and 30g/100ml for the three salt solutions. This is shown in Figure 7(d). Large values can be observed for the NaCl solution at the 450 nm, 550 nm, and 700 nm wavelengths (41 cm, 25 cm, and 12 cm respectively) than for the other two salts, with that of $CaCl_2$ being the lowest (0.3 cm, 0.27 cm, and 0.28 cm). Interpretation of this is that for a concentration change from 1g/100ml to 30g/100ml in a NaCl solution, there will be a reduction in transmission distance of 41 cm for blue light, while the red light will only suffer distance reduction of 12 cm. For KCl and $CaCl_2$ solutions, reduction in transmission distance between concentration of 1g/100ml and 30g/100ml is not much for the three wavelengths.

4.4. Results of the measurement of physiochemical parameters and determination of the metallic and chloride ions of the natural water bodies

We obtained the same results as [21] for the measured electrical conductivity, TDS, and TD salt of each sample of the seven water bodies. The Atlantic Ocean (AO) has the highest value of conductivity, TDS and TD salt,

followed by the Lagos lagoons. The rivers and Epe Lagoon are physically far away from the AO; hence their conductivity, TDS and TD salt are relatively low.

Table 4 shows the results of the measured salt ions and salinity of the water bodies. It shows the concentration of the metallic and chloride ions present in each of the water bodies. The salinity values in the table were calculated from the concentration of the chloride ions according to equation (1). AO has the highest amount of metallic ions and chloride ion. This makes the AO to have the highest salinity among them which translates to high conductivity level and will cause absorption of visible light.

Table 4. Measured salt ions and salinity of the selected water bodies of Southwest Nigeria.

Water Samples	Na^+ (ppm)	K^+ (ppm)	Ca^{2+} (ppm)	Cl^- (mg/L)	Salinity (ppt)
Ogbese River	61.400	72.000	20.840	29.150	0.053
Ala River	64.100	60.800	32.060	36.440	0.066
Epe Lagoon	65.100	58.500	9.630	76.530	0.138
Apake River	62.800	57.500	68.940	120.260	0.217
Lagos Lagoon Lekki Phase1 (LLLP1)	55.300	81.500	52.910	2405.210	4.345
Lagos Lagoon Victoria Island (LLVI)	50.600	75.200	136.270	7798.723	14.090
Atlantic Ocean (AO)	72.500	64.700	384.770	22047.770	39.830

Figure 8 shows the plots of electrical conductivity, TDS and TD salt against concentration of chloride ions in the natural water bodies. There is a strong positive correlation between the chloride ion concentration and the conductivity, the TDS and the TD salt.

In Table 4, Ogbese River, Ala River, Apake River, and Epe Lagoon have low chloride ion (Cl^-) content, which translate to low salinity and hence, low conductivity values. LLVI and LLLP1 contain chloride ion concentration that are less than that of the AO but higher than those of the rivers.

Concerning sodium ions (Na^+), the rivers have values within 61 ppm and 65 ppm. The AO has the highest concentration (72.5 ppm), but surprisingly, the two Lagos lagoons which are not relatively far from the AO have values lower than those of the rivers (50.6 ppm and 55.3 ppm). More surprising is the value of LLVI, which is lower (50.6 ppm) despite being closer to the AO than LLLP1.

Considering the potassium ions (K^+), the water bodies have differing values with Apake River having the lowest value and LLLP1 having the highest value. For the calcium ions (Ca^{2+}), Ogbese and Ala rivers have low values, Apake and LLLP1 have moderate values but Epe Lagoon has an extremely low value. A striking observation is that of the LLVI and the AO that have high values. The LLVI empties its contents directly into the AO. The AO, apart from having the highest Na+ concentration, also has the highest Ca^{2+} concentration among the three.

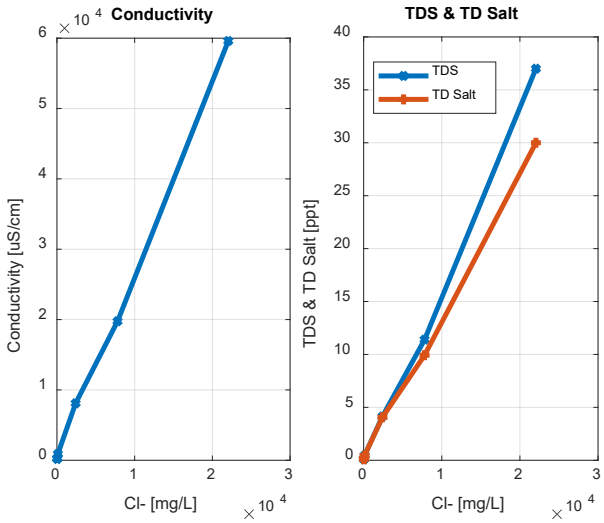

Fig. 8. Plot of electrical conductivity, TDS and TD Salt against chloride ion concentration in the water bodies.

4.5. Absorbance measurement of the water bodies

We obtained similar absorbance spectra for the water bodies as obtained by [21], and they are shown in Figure 9. The AO and the Lagos lagoons have higher absorbance spectra than those of Apake River, Epe Lagoon, Ala River and Ogbese River. The absorbance spectra of the water bodies bear a resemblance to that of the NaCl and KCl solutions obtained in this work as well as of the table salt water obtained in [20].

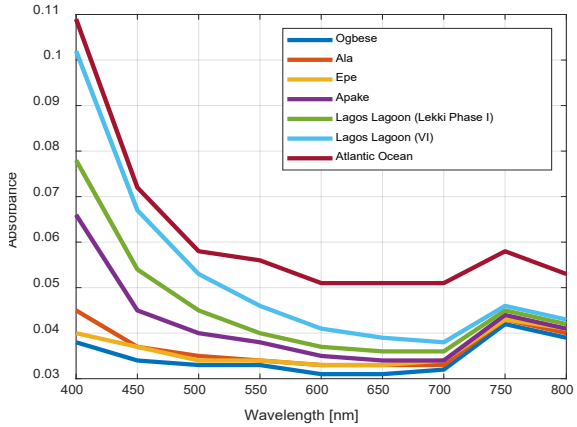

Fig. 9. Absorbance spectra of the water bodies between 400 nm – 800 nm.

Figure 10 shows the computed average absorbance of each of the water bodies following equation (5). In this case too, there are nine (9) wavelengths of measurement.

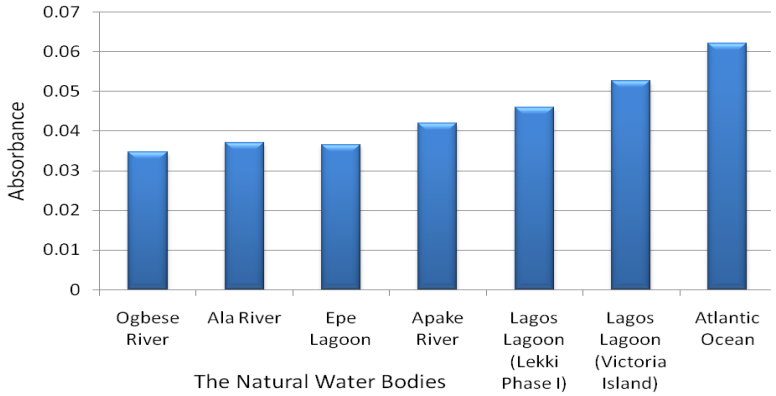

Fig. 10. Computed average absorbance of the seven water bodies.

The AO and the Lagos lagoons have higher average absorbance than Apake River, Epe Lagoon, Ala River and Ogbese River. The AO has the highest concentration of Na^+, Ca^{2+}, and the Cl^-. This all add up to its very high salinity and absorbance. Though Cl^- concentration has a direct bearing on the salinity, the absorbance of the water bodies does not only depend on the Cl^- concentration, but as well as on other contents of the waters, both inorganic and organic. We investigated any dependency between the average absorbance of the water bodies and the ions. Figure 11 shows the scatter plot of variation of the average absorbance with Na^+, K^+, Ca^{2+} and Cl^- concentrations of the water bodies. The horizontal axes for Ca^{2+} and Cl^- concentrations are in logarithmic scale.

Both the Na^+ and the K^+ show that the average absorbance has little or weak dependency on them. This agrees with literature that shows that there is little correlation of Na^+ and the K^+ with absorbance at low concentration levels [15, 16]. However, the Ca^{2+} and the Cl^- show the average absorbance to have some significant level of dependency on them, with the Cl^- showing higher degree of correlation. Pearson Correlation Coefficient was therefore computed in order to ascertain the level of correlation even though the sample sizes are few. The Pearson Correlation r_{xy} of N pairs of a paired data x, y, of a sample is defined as in equation (9):

$$r_{xy} = \frac{\sum_{i=1}^{N}(x_i-\bar{x})(y_i-\bar{y})}{\sqrt{\sum_{i=1}^{N}(x_i-\bar{x})^2}\sqrt{\sum_{i=1}^{N}(y_i-\bar{y})^2}} \quad (9)$$

where $\bar{x}$ and $\bar{y}$ are the mean of the paired data x_i, y_i respectively.

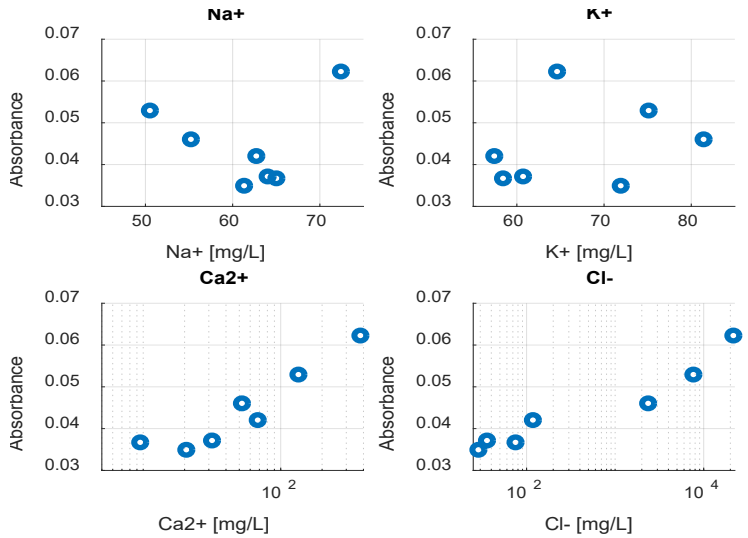

Fig. 11. Variation of the average absorbance with Na^+, K^+, Ca^{2+} and Cl^- concentrations of the water bodies.

Table 5 shows the obtained correlation coefficients between each of the ion concentration and the average absorbance of the water bodies.

Table 5. Correlation coefficients between each ion concentration and the average absorbance of the water bodies.

Ion conc. with Average Absorbance	Pearson Correlation Coefficient
Na^+	0.104
K^+	0.2492
Ca^{2+}	0.9239
Cl^-	0.9299

For the water bodies, their average absorbance shows a low positive correlation with Na^+ and K^+ concentrations, with K^+ having higher value compared to Na^+. However, a high positive correlation with Ca^{2+} and Cl^- can be observed, with the Cl^- having the highest correlation coefficient of +0.9299 with the average absorbance. Therefore, the Atlantic Ocean may be difficult for visible light communication at a very high data rate because its high chloride ion content translates to high salinity and conductivity level, and coupled with its high calcium ion content may cause considerable absorption of visible light.

5. CONCLUSIONS

This research investigated the transmission of visible light in samples of single-salt solutions of sodium, potassium and calcium chloride with varying concentrations via spectroscopy, and its attenuation effect on UWOC. In addition, the research investigated seven selected natural water bodies in Southwest Nigeria for presence of sodium, potassium, calcium and chloride ions, and effects on transmission of visible light in them.

Results showed that conductivity, salinity and absorbance increase with salt concentrations for all the three single-salt solutions. It is known that the absorbance of pure water is low in the blue-green wavelength, however; findings from this work revealed that the effects of absorption with salt concentrations are more pronounced at blue wavelengths than at red wavelengths for sodium chloride and potassium chloride solutions. For calcium chloride solution, the absorbance increases towards the green-red wavelength, and attenuation is more pronounced in it than in sodium and potassium chloride solutions.

Simulation of performance of UWOC in saline water shows that achievable maximum link distance reduces with increase in salinity, varies with wavelength, and is dependent on the type of salt. Lower maximum link distances were obtained with calcium chloride water than with sodium and potassium chloride waters. Red light, green light and blue light will travel best in sodium, potassium and calcium chloride waters respectively.

For the natural water bodies, the salinity of the Atlantic Ocean is the highest as it has the highest concentration of sodium, calcium and chloride ions. This causes high absorption of light and therefore the water may not be so suitable for underwater visible light communication at a very high data rate. The lagoons have moderate levels of salinity, and the rivers have low salinity compared to the ocean and the lagoons due to their low chloride ion concentration.

From this work, it is further established that in salty water, salinity is not strictly dependent on the amount of metallic ions (cations) the water contains but on the amount of chloride ion present. Also, the absorbance of visible light, among other factors, has dependency on the calcium ion and chloride ion concentrations, but less dependency on potassium and sodium ions. Hence, salty water that contains more calcium chloride salts than sodium chloride and potassium chloride salts may not be suitable for long distance and high data rate UWOC. Most seawater in the world contains more of sodium chloride than other salts thereby enabling UWOC in them.

Funding: *This research was funded by the authors and received no external funding.*

Data Availability Statement: *All data used and analyzed in this research are of the authors and are shown in the article. The absorbance data are available from the authors on reasonable request.*

Acknowledgments: *The authors thank the Department of Electrical and Electronics Engineering, of the Federal University of Technology Akure, Nigeria, for providing some of the facilities used in the absorbance measurement. Furthermore, appreciation to Mr. Olabisi Ajayi for the production of the salts and measurement of their ion contents*.

Conflicts of Interest: *The authors declare no conflicts of interest.*

REFERENCES

[1] Xu, J., Underwater wireless optical communication: Why, what, and how?, Chinese Optics Letters, vol. 17, no. 10, 2019, art. no. 100007.

[2] Jasman, F., Green, R.J., Monte Carlo simulation for underwater wireless communications, Proceedings of the IEE 2013 2nd International Workshop on Optical Wireless Communications (IWOW), 2013, p. 113-117.

[3] Zeng, F., Fu, S., Zhang, H., Dong, Y., Cheng, J., A survey of underwater optical wireless communications, IEEE Communication Survey and Tutorials, vol. 19, no. 1, 2017, pp. 204–238.

[4] Tang, S., Dong, Y., Zhang, X., Impulse response modeling for underwater wireless optical communication links, IEEE Transactions on Communications, vol. 62, no. 1, 2014, pp. 226-234.

[5] Liu, C., Liang, X., Ponte, R.M., Vinogradova, N., Wang, O., Vertical redistribution of salt and layered changes in global ocean salinity, Nature Communications, vol. 10, no. 1, 2019, pp. 1–8.

[6] Kumar, S., Prince, S., Aravind, J.V., Kumar, G.S., Analysis on the effect of salinity in underwater wireless optical communication, Marine Geo-resource and Geo-technology, vol. 38, 2019, pp. 291–301.

[7] Tian, P., Chen, H., Wang, P., Liu, X., Chen, X., Zhou, G., Zhang, S., Lu, J., Qiu, P., Qian, Z., Zhou, X., Fang, Z., Zheng, L., Liu, R., Cui, X., Absorption and scattering effects of Maalox, chlorophyll, and sea salt on a micro-LED-based underwater wireless optical communication, Chinese Optical Letters, vol. 17, no. 10, 2019, pp. 100010.

[8] Wozniak, B., Dera, J., Light Absorption in Sea Water, Springer, Berlin, Germany, 2007.

[9] Bernotas, M., Nelson, C., Probability density function analysis for optimization of underwater optical communications systems, Proceedings of OCEANS 2015-MTS/IEEE Washington, USA, 2015, pp. 1–8.

[10] Pegau, W.S., Gray, D., Zaneveld, J.R.V., Absorption and attenuation of visible and near-infrared light in water: dependence on temperature and salinity, Applied Optics, vol. 36, 1997, pp. 6035–6046.

[11] Gadani, D.H., Rana, V.A., Bhatnagar, S.P., Prajapati, A.N., Vyas, A.D., Effect of salinity on the dielectric properties of water, Indian Journal of Pure and Applied Physics, vol. 50, no. 6, 2012, pp. 405–410.

[12] Zhang, X., Hu, L., He, X., Scattering by pure seawater: Effect of salinity, Optical Express, vol. 17, no. 7, 2009, pp. 5698–5710.

[13] Ravisankar, M., Reghunath, A.T., Effect of dissolved NaCl, $MgCl_2$, and Na_2S0_4 in sea water on the optical attenuation in the region from 430 to 630 nm, Applied Optics, vol. 27, no. 18, 1988, pp. 3887–3894.

[14] Kumar, S., Prince, S., Kumar, G.S., Investigation on effects of system parameters on transmission depth in underwater wireless optical communication. Photonic Network Communications, vol. 41, 2021, pp. 163–176.

[15] Peters, R., Using spectra measurements to differentiate between aqueous NaCl and aqueous KCl in dual salt-solutions, Master's Thesis in the Department of Chemical and Biological Engineering, University of Saskatchewan, Saskatoon, 2016.

[16] Peters, R.D., Noble, S.D., Using near infrared measurements to evaluate NaCl and KCl in water, Journal of Near Infrared Spectroscopy, vol. 27, no. 2, 2019, pp. 147–155.

[17] Han, X., Peng, Y., Zhang, Y., Ma, Z., Wang, J., Research on the attenuation characteristics of some inorganic salts in seawater, Journal of the European Optical Society Rapid Publications, vol. 10, 2015, pp. 15045-1 - 15045-5.

[18] Wang, C.C., Tan, J.Y., Liu, L.H., Wavelength and concentration-dependent optical constants of NaCl, KCl, $MgCl_2$, $CaCl_2$, and Na_2SO_4 multi-component mixed-salt solutions, Applied Optics, vol. 56, no. 27, 2017, pp. 7662 – 7671.

[19] Ojediran, O.A., Ponnle, A.A., Oyetunji, S.A., Attenuation effect of saline water on performance of underwater wireless optical communication within the visible light range, Proceedings of 2021 SEET Annual Conference of Federal University of Technology, Akure, Nigeria, 2021, pp. 472 – 489.

[20] Ojediran, O.A., Ponnle, A.A., Oyetunji, S.A., Experimental study on transmission of visible light in table salt water and effect on underwater wireless optical communication, European Journal of Electrical Engineering and Computer Science, vol. 6, no. 2, 2022, pp. 25-32.

[21] Orjiekwe, C.L., Dumo, D.T., Chinedu, N.B., Assessment of water quality of Ogbese River in Ovia North-East Local Government area of Edo State, Nigeria, International Journal of Biological and Chemical Sciences, vol. 7, no. 6, 2013, pp. 2581-2590.

[22] Akinbile, C.O., Omoniyi, O., Quality assessment and classification of Ogbese river using water quality index (WQI) tool, Sustainable Water Resources Management, vol. 4, 2018, pp.1023-1030.

[23] Akagha, S.C., Nwankwo, D.I., Yin, K., Dynamics of nutrient and phytoplankton in Epe Lagoon, Nigeria: possible causes and consequences of reoccurring cyanobacterial blooms, Applied Water Science, vol. 10, no. 5, 2020, pp.1-16.

[24] Ojediran, O.A., Ponnle, A.A., Oyetunji, S.A., Study on transmission of visible light in selected water bodies of Southwest Nigeria for underwater wireless optical communication, Journal of Engineering Advancements, vol. 4, no. 3, 2023, pp. 80–89.

[25] Chai, B.-h., Zheng, J.-m., Zhao, Q., Pollack, G.H., Spectroscopic studies of solutes in aqueous solution, Journal of Physical Chemistry A, vol. 112, no. 11, 2008, pp. 2242-2247.

[26] Mullen, B.C., Free-space optical communications underwater, Advanced Optical Wireless Communication Systems, Cambridge University Press, 2012.

[27] Mohammed, E., Farshad, M., Uysal, M., Channel modeling and performance characterization of underwater visible light communications, Proceedings of IEEE International Conference on Communication Workshops, 2018, pp. 1-5.

[28] Ajibodu, F.A., Ojo, B.A., Performance evaluation of the maximum achievable bit rate of a next generation TWDM passive optical network, American Journal of Engineering Research, vol. 5, no. 1, 2016, pp. 104 -109.

[29] PG Instruments, FP910 Flame Photometer. Available online: https://www.pginstruments.com/product/fp910-flame-photometer (26.09.2023).

[30] A.O.A.C. 1990. Official methods of analysis of the AOAC, 15th edition. Methods 932.06, 925.09, 985.29, 923.03. Association of Official Analytical Chemists, Arlington, VA, USA.

[31] Ekundayo, F.O., Omiyale, F.B., Omomo, E.R., Flocculating properties of a bioflocculant purified from bacillus subtilis isolated from the stream sediments of Onyearugbulem market, Akure, Nigeria, Microbiology Research Journal International, vol. 8, no. 5, 2019, pp. 1-16.